ACS OMEGA

http://pubs.acs.org/journal/acsodf

Article

Strict Twice Iterative Optimization Strategy to Synthesize Ultrabright Fluorescent Carbon Dots for UV and pH Dual-Encryption Fluorescent Ink

Jiamei Xiang, Ruixue Li, Xiang Long, Shaogui Wu,* Jiayang Wang, and Zhuo Wang

Cite This: *ACS Omega* 2022, 7, 29952−29958

Read Online

ACCESS | Metrics & More | Article Recommendations | Supporting Information

ABSTRACT: In this work, ultrabright fluorescent carbon dots (U-CDs) were synthesized by using a strict twice iterative optimization strategy. Their relative photoluminescence (PL) quantum yield is close to 100%, exceeding most of the reported fluorescent CDs and greatly boosting the practical applications of fluorescent CDs in many fields. Then serving as fluorescent anti-counterfeiting ink was taken as an example to briefly introduce the application of the U-CDs. The PL emission of the U-CDs is quenched at the range of pH < 4 or pH > 11 and restored at the range of pH = 5−10. This pH-sensitive PL feature allows the U-CDs to be used as fluorescent ink for pH and UV dual information encryption. The written or printed information is invisible under daylight but visible under UV light. After acid treatment or alkali treatment, the information is invisible even under a UV lamp but visible after neutralization treatment. This work provides a standardized scheme for optimizing the synthesis conditions of fluorescent CDs and paves the way for large-scale production of high-performance fluorescent CDs.

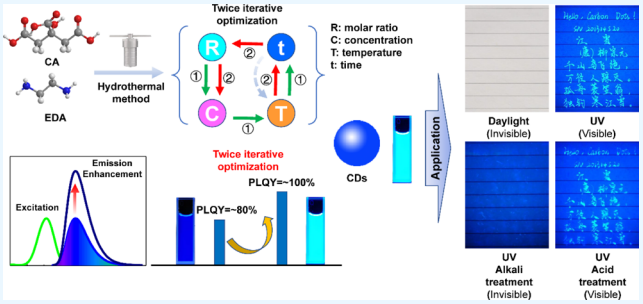

1. INTRODUCTION

Carbon dots (CDs), a new member of carbon materials family, are a class of novel carbon nanofluorescent materials.[1,2] Due to their low toxicity, low production cost, and easy preparation, CDs exhibit a wide range of application prospects in the fields of display equipment,[3−5] energy conversion,[6−8] bioimaging,[9−11] analytical detection,[12−15] and so forth. However, currently synthesized CDs mostly suffer from low photoluminescence (PL) quantum yield (QY), which hinders their practical applications. The PL mechanism of CDs remains in debate, inducing difficulties to the synthesis of CDs with a high PLQY. On the other hand, research on improving the PLQY of CDs is a hard work with huge workload, a long research time, and a high characterization cost, making it difficult to grasp accurate rules. It is well known that CDs synthesized by pure carbohydrates have poor PLQY (<10%),[16,17] while nitrogen doping can effectively improve the PLQY (10−40%).[18,19] Organic acids and organic amines are currently popular raw material combinations for CD synthesis, in which citric acid (CA) and ethylenediamine (EDA) are a famous combination that can synthesize CDs with a considerable PLQY (up to 60−80%).[20]

In this work, CA and EDA were also used as the precursors for the synthesis of fluorescent CDs. An iterative strategy is a computer programming idea, which takes the result of the previous calculation cycle as the initial value for the next calculation cycle until an optimal value is obtained.[21] In order to pursue the ceiling of fluorescent CDs, a twice iterative strategy is used to optimize the synthesis conditions of fluorescent carbon dots, such as CA and EDA molar ratio ($R_{CA/EDA}$), concentration (represented by the total amount of CA and EDA, denoted by n), reaction time (t), and temperature (T). Specifically, we carried out two rounds of optimizations on the four experimental parameters. The first round of optimization seeks their rough values, which were used as input values for the second round of optimization. Then the second round of optimization was conducted to find their optimal values. In order to reduce the experimental error, six parallel experiments were carried out at each experimental point in the second round of optimization to calculate the average and variance of PLQY. Based on large-scale experiments (thousands of spectra on hundreds of samples), we successfully synthesize ultra-bright CDs (U-CDs) with a relative PLQY close to 100%.

Furthermore, taking the use of anti-counterfeiting ink as an example, a practical application of U-CDs is introduced. U-CDs have excellent PL performance and maintain a considerable PL intensity even at a relative low concentration. Although the as-prepared U-CD solution is faint yellow under

Received: May 12, 2022
Accepted: August 9, 2022
Published: August 17, 2022

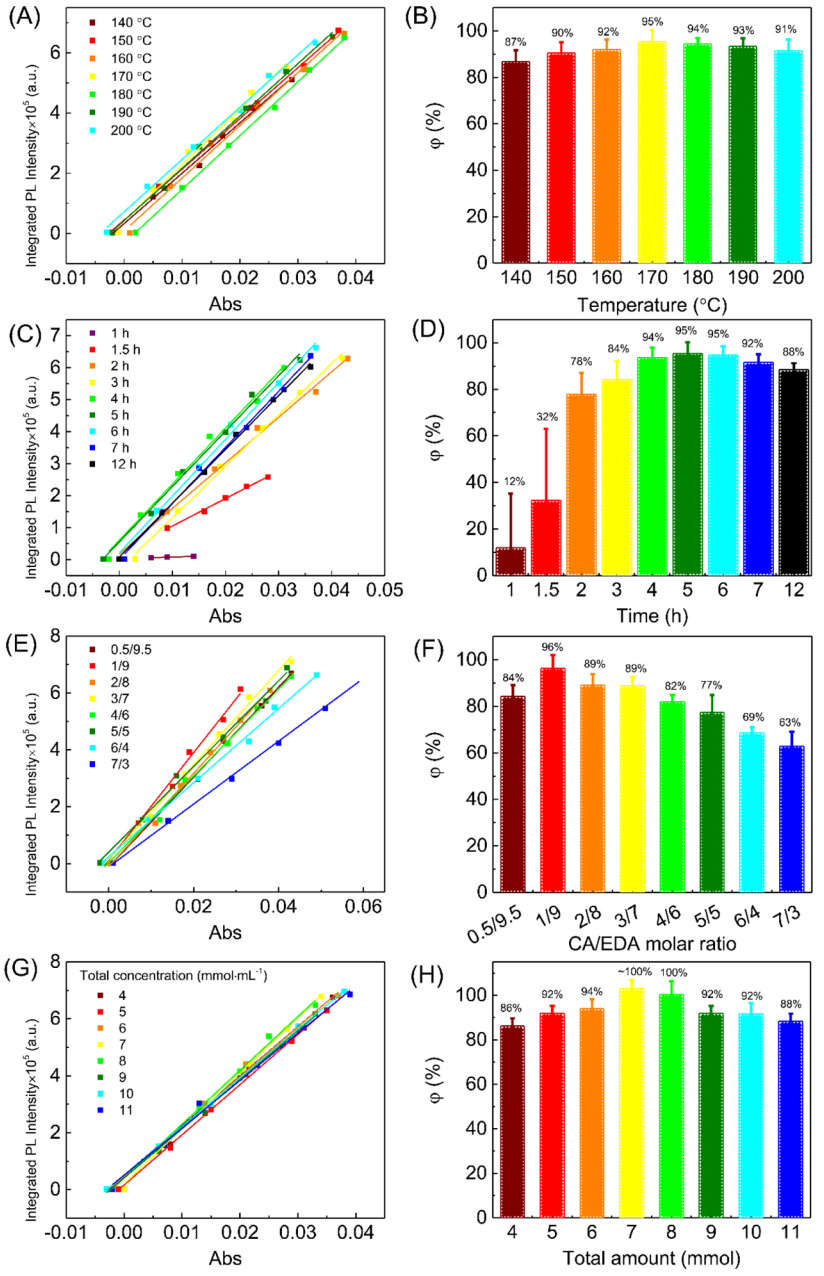

Figure 1. Result of the second round of optimization. (A) Fitting curves of integral PL intensity and absorbance for reaction temperature optimization. (B) Average PLQY as a function of reaction temperature; (C) fitting curves of integral PL intensity and absorbance for heating time. (D) Average PLQY a function of heating time; (E) fitting curves of integral PL intensity and absorbance for CA/EDA molar ratio optimization. (F) Average PLQY a function of CA/EDA molar ratio; (G) fitting curves of integral PL intensity and absorbance for the total amount of CA and EDA optimization. (H) Average PLQY as a function of the total amount of CA and EDA.

daylight, it is almost colorless after dilution, leaving no trace after writing or printing information on media such as paper. However, when exposed to a UV lamp, the written or printed information emits strong fluorescence for identification. Among all fluorescent CDs reported so far, the U-CDs are one of the few fluorescent inks with a real practical application value. Furthermore, the PL emission of the U-CDs is quenched under an acid (pH < 4) or alkali (pH > 11) environment but remains stable in a near-neutral environment (pH = 5−10), which allows the U-CDs be applicated as a fluorescent ink for pH and UV dual information encryption. This work provides an idea for optimizing the synthesis conditions of fluorescent CDs and also promotes the practical applications of CDs.

2. EXPERIMENT

2.1. Instruments and Reagents. A hydrothermal reactor (25 mL) was purchased from Anniu Technology Co., Ltd. An electric drying oven was purchased in Shanghai Lichen Technology Co., Ltd. UV−vis spectra were measured using a Shunyuhengping 756 PC UV−vis spectrophotometer, and fluorescence spectra were determined using a Shanghai Lengguang F98 fluorescence spectrophotometer.

Quinine sulfate was purchased from Shanghai Aladdin Biochemical Technology Co., Ltd. Chemical reagents such as CA and EDA were purchased from Tianjin Comiou Chemical reagent Co., Ltd. The experimental water was self-made secondary distilled water.

https://doi.org/10.1021/acsomega.2c02949
ACS Omega 2022, 7, 29952−29958

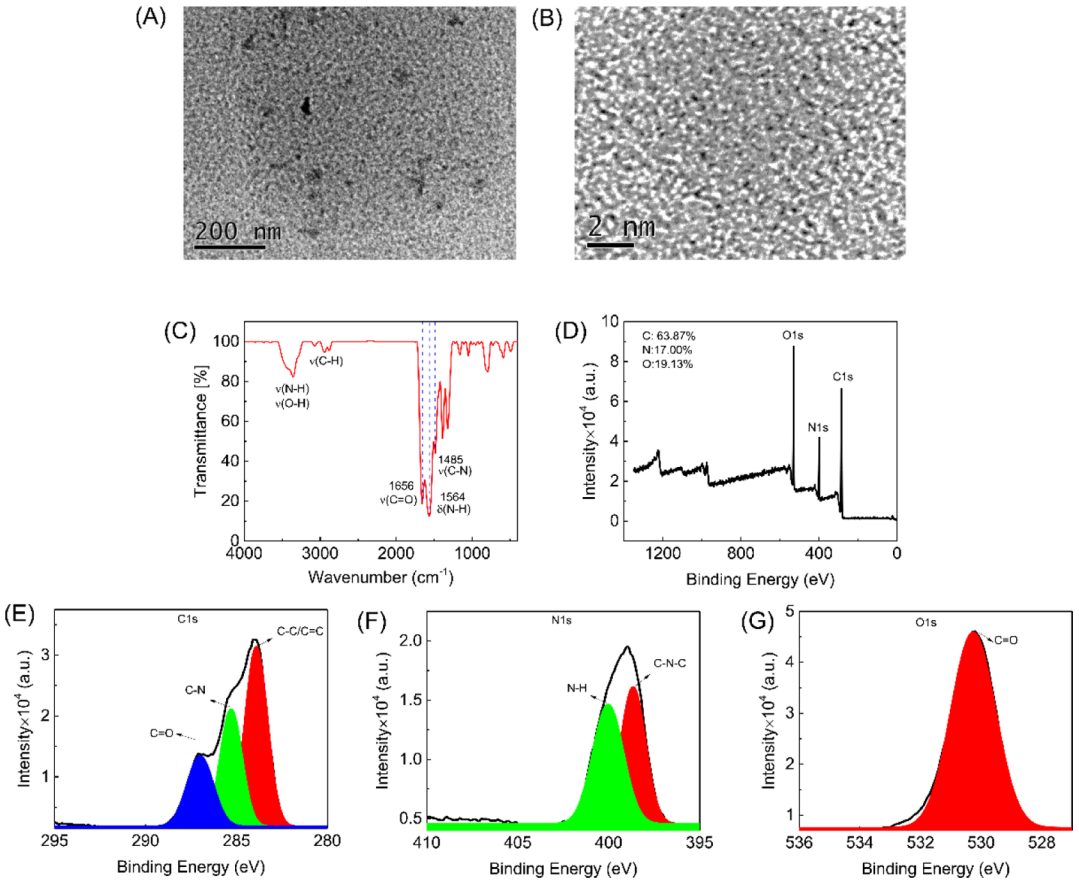

Figure 2. Structural characterization of the U-CDs. (A) TEM image. (B) Zoom-in image of a particle in 2 nm resolution. (C) FT-IR spectrum. (D) Wide-scan XPS spectrum of U-CDs. (E−G) High-resolution XPS spectra of C 1s, N 1s, and O 1s, respectively.

2.2. Synthesis of U-CDs. Since the discovery of CDs in 2004,[22] various methods have been developed for preparing CDs.[23−25] In this work, the U-CDs were synthesized by the conventional hydrothermal method.[26,27] The twice iterative optimization strategy was used to optimize the experimental parameters. CA and EDA were used as raw materials with a controlled molar ratio of CA to EDA in the range of 0.5/9.5−7/3. The reaction temperature was optimized from 140 to 200 °C, and the reaction time was varied from 1 to 12 h in order to control the extent of graphitization. Typically, 1 mmol CA and 9 mmol EDA were dissolved into 10 mL of secondary distilled water. Then the solution was kept at 170 °C for 5 h in a 25 mL Teflon-lined stainless-steel autoclave. After that, the reactor was cooled naturally in the oven. The product solution was subjected to centrifugation at 10,000 rpm for 10 min to remove the insoluble solid and then stored as a stock solution in a 4 °C refrigerator for standby. The details about relative PLQY determination can be found in Figure S1.

2.3. Structural Characterization. Fourier transform infrared spectroscopy (FT-IR): the U-CD solution was dried in a vacuum oven at 60 °C. The obtained U-CD powder was mixed with KBr in the ratio of 1:100, grinded, and pressed, and then FT-IR measurements were carried out with a scanning range of 4000−400 cm^{-1}. X-ray photoelectron spectroscopy (XPS): the surface composition of dried U-CDs was determined using a Geneis 60s X-ray photoelectron spectrometer with C 1s (284.6 eV) as the internal standard. Transmission electron microscopy (TEM): the U-CD solution was dropped on a copper wire. After drying under light, the morphology of U-CDs was observed using a Hitachi H-7650 electron microscope. In addition, quinine sulfate was employed as a standard reference to estimate the relative PLQY of U-CDs.[28,29] The details of determination of relative PLQY can be found in the Supporting Information.

3. RESULTS AND DISCUSSION

3.1. Synthesis of Ultra-Bright Fluorescent CDs. In order to synthesize ultra-bright fluorescent CDs, we carried out a strict twice iterative optimization on the four synthesis conditional parameters, such as $R_{CA/EDA}$, n, t, and T. Figure 1 displays the final result of the second round of optimization. With the increase of temperature, the PLQY first increases and then decreases, and the maximum (PLQY = 95 ± 5%) appears near 170 °C (Figure 1A,B), suggesting that 170 °C is a favorable temperature for the synthesis of high PLQY U-CDs, which is different from the synthesis temperature of 200 °C recorded in the literature.[30] Obviously, a high temperature (>170 °C) facilitates the carbonization of raw materials, but it is not useful to enhance the PLQY of CDs synthesized by organic acids and organic amines. Figure 1C,D displays the result from time optimization. With the increase of heating time, the PLQY reaches the maximum (95 ± 5%) at the time of 5 h. Prolonging the heating time (>5 h) might also increase the carbonization degree but contributes little to enhancing the PLQY of CDs. It implies that the PLQY of U-CDs might be independent of the carbonization degree of raw materials. The composition of the raw materials plays an important role in CD synthesis. Figure 1E,F shows the results from $R_{CA/EDA}$

https://doi.org/10.1021/acsomega.2c02949
ACS Omega 2022, 7, 29952−29958

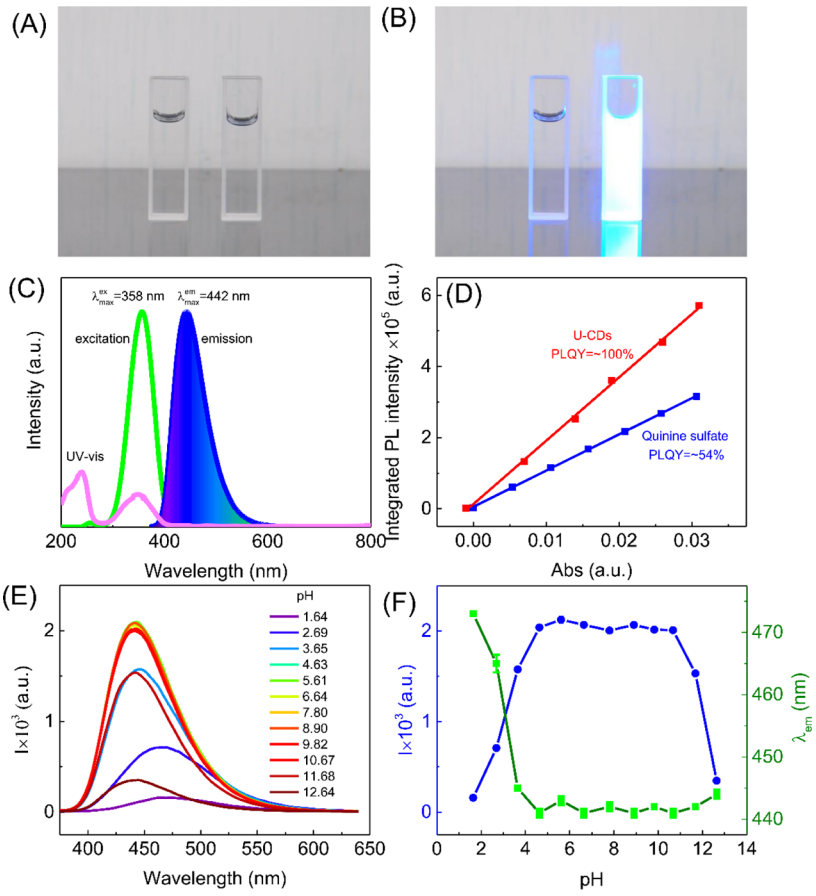

Figure 3. Optical properties of the U-CDs. (A) Water (left) and the U-CD (right) samples in the daylight. (B) Water (left) and the U-CD (right) samples under UV light. (C) UV−vis absorption spectrum (red), excitation spectrum (green), and emission spectrum (blue) of the U-CDs. (D) Fitting curve of integrated PL intensity and UV−vis absorbance. (E) Emission spectra and (F) PL intensity and emission wavelength as functions of solvent pH value.

optimization, where the n was fixed at 10 mmol and the $R_{CA/EDA}$ was changed from 0.5/9.5 to 7/3. It is interesting to find that the highest PLQY appears at $R_{CA/EDA}$ = 1/9. Increasing the ratio of EDA can enhance the PLQY, indicating that the nitrogen content in U-CDs has a great influence on the PL performance of U-CDs. When $R_{CA/EDA}$ is large, CA is surplus, while most of EDA is converted into U-CDs as much as possible. The CA molecules contain a large amount of carboxyl groups, which absorb the light at the excitation wavelength but have no emission ability, resulting in the reduction of PLQY. When $R_{CA/EDA}$ is very small, EDA is surplus, and most of CA can be transformed into U-CDs as much as possible, which is useful for enhancing the PLQY of U-CDs, while the utilization rate of raw materials is low. The total amount (n) of CA and EDA is used to control the concentration of reactants and products. Figure 1G,H indicates that the optimal reaction conditions are temperature = 170 °C, time = 5 h, CA/EDA ratio = 1/9, and total amount = 7 mmol, where the product U-CDs have the highest relative PLQY (~100%), which were used in the following experiments.

3.2. Structural Characterization. TEM analysis was conducted to study the morphology and the average size of the synthesized U-CDs. As shown in Figure 2A, one can see that these particles are not regular spherical, and the size distribution ranges from nano to micron. These features are not in line with the morphology (spherical) and size of conventional CDs (<10 nm). In addition, there are not many particles observed under TEM, implying that these particles might be not the only substance with PL activity. Figure 2B shows a TEM image in high resolution. No ordered lattice is observed in the particle, suggesting that the U-CDs do not have a core of the graphene structure. It is speculated that these particles might be disordered flocs formed by CA and EDA.

The functional groups of U-CDs were characterized by FT-IR, as shown in Figure 2C. The peak at 3700−3200 cm^{-1} is the O−H stretching vibration peak; the peak at 3500−3300 cm^{-1} is the N−H stretching vibration peak; the peak at 2923−2853 cm^{-1} is the C−H stretching vibration peak; the peak at 1656 cm^{-1} is the C═O (amide I) stretching vibration peak;[31] the peak at 1564 cm^{-1} is the bending vibration peak of the N−H (amide II) on the amide bond;[32] the peak at 1485 cm^{-1} is the C−N (amide III) stretching vibration peak.[33] The three peaks are characteristic absorption peaks of the amide bond. In addition, the U-CDs may also contain $-NH_2$, −OH, and −COOH functional groups. The chemical composition and elemental composition of U-CDs were analyzed by XPS. Figure 2D displays a wide-scan XPS spectrum of U-CDs, which shows three characteristic binding energy peaks, namely, C 1s (284.18 eV), N 1s (399.11 eV), and O 1s (530.22 eV), indicating that the U-CDs mainly contain three elements, C, N, and O, and the relative content ratio of C/N/O is 63.87%:17.00%:19.13%. Figure 2E displays the XPS spectrum for C 1s, which has three characteristic carbon peaks, 283.91

https://doi.org/10.1021/acsomega.2c02949
ACS Omega 2022, 7, 29952−29958

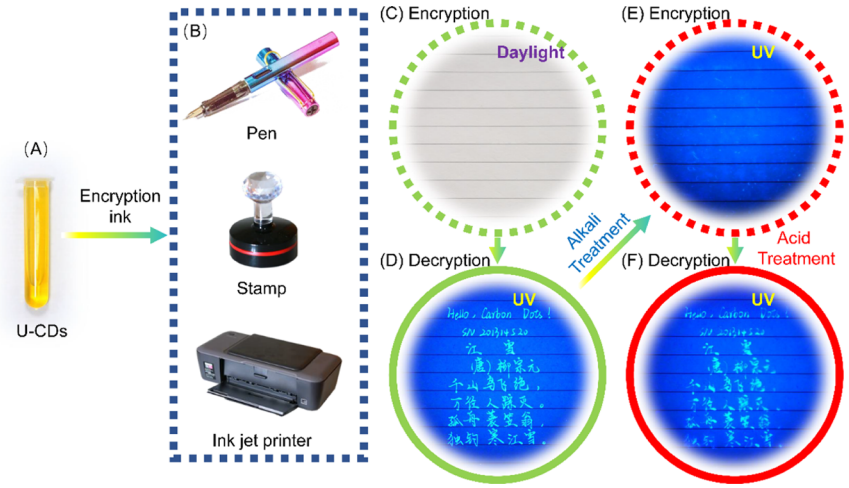

Figure 4. U-CDs can be used as a UV and pH double-encryption fluorescent ink. Diluted U-CD solution (A) can be used as ink for pens, stampers, and inkjet printers (B). Information written by U-CD ink is invisible under sunlight (C) and visible under UV light (D). The information disappears after alkali treatment (E) and reappears after acid treatment (F).

eV (C−C/C═C), 285.29 eV (C−N), and 287.03 eV (C═O).[34] Figure 2F is the N 1s spectrum, and two subpeaks of 398.65 eV (C−N−C) and 400.03 eV (N−H) can be resolved. Figure 2G is the O 1s spectrum; only one characteristic peak is observed at 530.24 eV (C═O).

3.3. Optical Properties. Figure 3A displays a distilled water sample (left) and a U-CD sample with a concentration of ∼5 μg/mL (right) under daylight. One can see that the U-CD sample is almost colorless and transparent, which shows no difference from the water sample. However, when both samples are exposed to UV light (365 nm), and the U-CD sample emits strong fluorescence, which is in sharp contrast with the water sample, as shown in Figure 3B. The UV−vis absorption, excitation, and emission spectra of the U-CDs are shown in Figure 3C. The UV−vis absorption spectrum has two main absorption peaks at 240 and 360 nm. The one at 360 nm is basically coincident with the excitation peak, which is the characteristic absorption peak of the U-CDs, which is contributed from the n → π* electronic transition.[31,35] The excitation and emission spectra are basically symmetrical. The maximum excitation and emission wavelengths are 358 nm and 442 nm, respectively. If quinine sulfate is used as the standard reference (PLQY = ∼54%), one can estimate the PLQY of final U-CDs to be ∼100%, as shown in Fig.3D. Furthermore, the influence of pH on the optical activities of U-CDs was investigated. As shown in Figure 3E,F, with the increase of pH value, the PL intensity of U-CDs first increases and then decreases, and a platform appears in the range of pH = 5−11. It is obvious that the PL emission of U-CDs is quenched in an acidic (pH < 4) or alkaline (pH > 10) environment. Note that this PL quenching phenomenon can be reduced by changing the pH value of the solution. On the other hand, when the pH value increases from 2 to 4, the emission wavelength has obvious blue shift.

3.4. UV and pH Double-Encryption Fluorescent Ink. As mentioned above, the PL emission of U-CDs can be quenched in a strong acid or alkali environment but restored when the pH is tuned to the range of pH = 5−11. This feature allows the U-CDs to be used as UV and pH double-encryption fluorescent ink. The as-prepared U-CD solution is diluted by 1:1 with water, and the diluted solution (Figure 4A) can serve as encryption fluorescent ink for ordinary pens, stampers, inkjet printers, and so forth (Figure 4B). The information written or printed is invisible under sunlight (Figure 4C) and is clearly seen under UV light (Figure 4D). When the paper is soaked by 1 M NaOH solution, the information disappears again even under UV light, as shown in Figure 4E. After a simple acid treatment by 1 M HCl solution, the information appears again (Figure 4F). Thus, the U-CDs can be used as a UV and pH double-encryption fluorescent ink.

4. CONCLUSIONS

In this work, based on large-scale experiments, U-CDs were synthesized by using a strict twice iterative optimization strategy. Their relative PLQY is close to 100%, exceeding those of most of the reported fluorescent CDs. The maximum excitation and emission wavelengths are 358 and 442 nm, respectively. In addition, the PL emission of the U-CDs is quenched at very low and very high pH but remains stable in a near-neutral environment. This feature allows the U-CDs be applicated as a fluorescent anti-counterfeiting ink for pH and UV dual information encryption. This work provides a solution for optimizing the synthesis conditions of fluorescent CDs and also promotes the practical applications of CDs.

■ ASSOCIATED CONTENT

Supporting Information

The Supporting Information is available free of charge at https://pubs.acs.org/doi/10.1021/acsomega.2c02949.

Determination of relative PLQY using quinine sulfate as a standard reference and result of primary optimization (PDF)

■ AUTHOR INFORMATION

Corresponding Author

Shaogui Wu − *College of Chemistry and Materials Science, Sichuan Normal University, Chengdu 610066, China;* orcid.org/0000-0002-0193-8741; Email: shaoguiwu@sicnu.edu.cn

Authors

Jiamei Xiang − *College of Chemistry and Materials Science, Sichuan Normal University, Chengdu 610066, China*

https://doi.org/10.1021/acsomega.2c02949
ACS Omega 2022, 7, 29952−29958

Ruixue Li − *College of Chemistry and Materials Science, Sichuan Normal University, Chengdu 610066, China*
Xiang Long − *College of Chemistry and Materials Science, Sichuan Normal University, Chengdu 610066, China*
Jiayang Wang − *Department of Resources & Environment, Chengdu University of Information Technology, Chengdu 610041, China*
Zhuo Wang − *Department of Resources & Environment, Chengdu University of Information Technology, Chengdu 610041, China*

Complete contact information is available at:
https://pubs.acs.org/10.1021/acsomega.2c02949

Notes

The authors declare no competing financial interest.

■ ACKNOWLEDGMENTS

This work was supported by the Project of Science and Technology Department of Sichuan Province, China (no. 21RKX0358).

■ REFERENCES

(1) Sun, Y.; Zhou, B.; Lin, Y.; Wang, W.; Fernando, K. S.; Pathak, P.; Meziani, M. J.; Harruff, B. A.; Wang, X.; Wang, H.; Luo, P. G.; Yang, H.; Kose, M. E.; Chen, B.; Veca, L. M.; Xie, S.-Y. Quantum-sized carbon dots for bright and colorful photoluminescence. *J. Am. Chem. Soc.* **2006**, *128*, 7756−7757.
(2) Kang, Z.; Lee, S.-T. Carbon dots: advances in nanocarbon applications. *Nanoscale* **2019**, *11*, 19214−19224.
(3) Jiang, K.; Sun, S.; Zhang, L.; Lu, Y.; Wu, A.; Cai, C.; Lin, H. Red, Green, and Blue Luminescence by Carbon Dots: Full-Color Emission Tuning and Multicolor Cellular Imaging. *Angew. Chem., Int. Ed.* **2015**, *127*, 5450−5453.
(4) Li, Z.; Wang, L.; Li, Y.; Feng, Y.; Feng, W. Frontiers in carbon dots: design, properties and applications. *Mater. Chem. Front.* **2019**, *3*, 2571−2601.
(5) Wang, H.; Sun, C.; Chen, X.; Zhang, Y.; Colvin, V. L.; Rice, Q.; Seo, J.; Feng, S.; Wang, S.; Yu, W. Y. Excitation wavelength independent visible color emission of carbon dots. *Nanoscale* **2017**, *9*, 1909−1915.
(6) Sun, D.; Ban, R.; Zhang, P.-H.; Wu, G.-H.; Zhang, J.-R.; Zhu, J.-J. Hair fiber as a precursor for synthesizing of sulfur- and nitrogen-co-doped carbon dots with tunable luminescence properties. *Carbon* **2013**, *64*, 424−434.
(7) Wang, H.; Sun, P.; Cong, S.; Wu, J.; Gao, L.; Wang, Y.; Dai, X.; Yi, Q.; Zou, G. Nitrogen-doped carbon dots for "green" quantum dot solar cells. *Nanoscale Res. Lett.* **2016**, *11*, 27.
(8) Luo, H.; Guo, Q.; Szilágyi, P. Á.; Jorge, A. B.; Titirici, M.-M. Carbon dots in solar-to-hydrogen conversion. *Trends Chem.* **2020**, *2*, 623−637.
(9) Kim, K. W.; Choi, T.-Y.; Kwon, Y. M.; Kim, J. Y. H. Simple synthesis of photoluminescent carbon dots from a marine polysaccharide found in shark cartilage. *Electron. J. Biotechnol.* **2020**, *47*, 36−42.
(10) Arumugam, S. S.; Xuing, J.; Viswadevarayalu, A.; Rong, Y.; Sabarinathan, D.; Ali, S.; Agyekum, A. A.; Li, H.; Chen, Q. Facile preparation of fluorescent carbon quantum dots from denatured sour milk and its multifunctional applications in the fluorometric determination of gold ions, in vitro bioimaging and fluorescent polymer film. *J. Photochem. Photobiol., A* **2020**, *401*, 112788.
(11) Guo, R.; Liu, X.; Wen, B.; Liu, F.; Meng, J.; Wu, P.; Wu, J.; Li, Q.; Mai, L. Engineering mesoporous structure in amorphous carbon boosts potassium storage with high initial coulombic efficiency. *Nano-Micro Lett.* **2020**, *12*, 148.
(12) Wang, B.-B.; Jin, J.-C.; Xu, Z.-Q.; Jiang, Z.-W.; Li, X.; Jiang, F.-L.; Liu, Y. Single-step synthesis of highly photoluminescent carbon dots for rapid detection of Hg2+ with excellent sensitivity. *J. Colloid Interface Sci.* **2019**, *551*, 101−110.
(13) Wang, B.; Chen, Y.; Wu, Y.; Weng, B.; Liu, Y.; Lu, Z.; Li, C. M.; Yu, C. Aptamer induced assembly of fluorescent nitrogen-doped carbon dots on gold nanoparticles for sensitive detection of AFB1. *Biosens. Bioelectron.* **2016**, *78*, 23−30.
(14) Xu, Q.; Pu, P.; Zhao, J.; Dong, C.; Gao, C.; Chen, Y.; Chen, J.; Liu, Y.; Zhou, H. Preparation of highly photoluminescent sulfur-doped carbon dots for Fe(iii) detection. *J. Mater. Chem. A* **2015**, *3*, 542−546.
(15) Da, L. T.; Pardo-Avila, F.; Xu, L.; Silva, D. A.; Zhang, L.; Gao, X.; Wang, D.; Huang, X. H. Bridge helix bending promotes RNA polymerase II backtracking through a critical and conserved threonine residue. *Nat. Commun.* **2016**, *7*, 11244.
(16) Hsu, P.-C.; Chen, P.-C.; Ou, C.-M.; Chang, H.-Y.; Chang, H.-T. Extremely high inhibition activity of photoluminescent carbon nanodots toward cancer cells. *J. Mater. Chem. B* **2013**, *1*, 1774−1781.
(17) Kumari, A.; Kumar, A.; Sahu, S. K.; Kumar, S. Synthesis of green fluorescent carbon quantum dots using waste polyolefins residue for Cu2+ ion sensing and live cell imaging. *Sens. Actuators, B* **2018**, *254*, 197−205.
(18) Zhu, S.; Song, Y.; Zhao, X.; Shao, J.; Zhang, J.; Yang, B. The photoluminescence mechanism in carbon dots (graphene quantum dots, carbon nanodots, and polymer dots): current state and future perspective. *Nano Res.* **2015**, *8*, 355−381.
(19) Iqbal, A.; Iqbal, K.; Xu, L.; Li, B.; Gong, D.; Liu, X.; Guo, Y.; Liu, W.; Qin, W.; Guo, H. Heterogeneous synthesis of nitrogen-doped carbon dots prepared via anhydrous citric acid and melamine for selective and sensitive turn on-off-on detection of Hg (II), glutathione and its cellular imaging. *Sens. Actuators, B* **2018**, *255*, 1130−1138.
(20) Kokorina, A. A.; Bakal, A. A.; Shpuntova, D. V.; Kostritskiy, A. Y.; Beloglazova, N. V.; De Saeger, S.; Sukhorukov, G. B.; Sapelkin, A. V.; Goryacheva, I. Y. Gel electrophoresis separation and origins of light emission in fluorophores prepared from citric acid and ethylenediamine. *Sci. Rep.* **2019**, *9*, 14665.
(21) Gleixner, A. M.; Steffy, D. E.; Wolter, K. Iterative refinement for linear programming. *Inf. J. Comput.* **2016**, *28*, 449−464.
(22) Xu, X.; Ray, R.; Gu, Y.; Ploehn, H. J.; Gearheart, L.; Raker, K.; Scrivens, W. A. Electrophoretic analysis and purification of fluorescent single-walled carbon nanotube fragments. *J. Am. Chem. Soc.* **2004**, *126*, 12736−12737.
(23) Roy, P.; Chen, P.-C.; Periasamy, A. P.; Chen, Y.-N.; Chang, H.-T. Photoluminescent carbon nanodots: synthesis, physicochemical properties and analytical applications. *Mater. Today* **2015**, *18*, 447−458.
(24) Li, L.; Wu, G.; Yang, G.; Peng, J.; Zhao, J.; Zhu, J.-J. Focusing on luminescent graphene quantum dots: current status and future perspectives. *Nanoscale* **2013**, *5*, 4015−4039.
(25) Li, H.; He, X.; Kang, Z.; Huang, H.; Liu, Y.; Liu, J.; Lian, S.; Tsang, C. H. A.; Yang, X.; Lee, S. T. Water-Soluble Fluorescent Carbon Quantum Dots and Photocatalyst Design. *Angew. Chem., Int. Ed.* **2010**, *49*, 4430−4434.
(26) Liu, Y.; Zhou, Q.; Li, J.; Lei, M.; Yan, X. Selective and sensitive chemosensor for lead ions using fluorescent carbon dots prepared from chocolate by one-step hydrothermal method. *Sens. Actuators, B* **2016**, *237*, 597−604.
(27) Liu, S.; Cui, J.; Huang, J.; Tian, B.; Jia, F.; Wang, Z. Facile one-pot synthesis of highly fluorescent nitrogen-doped carbon dots by mild hydrothermal method and their applications in detection of Cr(VI) ions. *Spectrochim. Acta, Part A* **2019**, *206*, 65−71.
(28) Kim, H. N.; Ren, W. X.; Kim, J. S.; Yoon, J. Fluorescent and colorimetric sensors for detection of lead, cadmium, and mercury ions. *Chem. Soc. Rev.* **2012**, *41*, 3210−3244.
(29) Wu, S.; Zhou, C.; Ma, C.; Yin, Y.; Sun, C. Carbon Quantum Dots-Based Fluorescent Hydrogel Hybrid Platform for Sensitive Detection of Iron Ions. *J. Chem.* **2022**, *2022*, 3737646.
(30) Li, M.; Yao, W.; Liu, J.; Tian, Q.; Liu, L.; Ding, J.; Xue, Q.; Lu, Q.; Wu, W. Facile synthesis and screen printing of dual-mode

luminescent NaYF4:Er,Yb (Tm)/carbon dots for anti-counterfeiting applications. *J. Mater. Chem. C* **2017**, *5*, 6512−6520.
(31) Zhang, Y.; Liu, X.; Fan, Y.; Guo, X.; Zhou, L.; Lv, Y.; Lin, J. One-step microwave synthesis of N-doped hydroxyl-functionalized carbon dots with ultra-high fluorescence quantum yields. *Nanoscale* **2016**, *8*, 15281−15287.
(32) Vallan, L.; Urriolabeitia, E. P.; Ruipérez, F.; Matxain, J. M.; Canton-Vitoria, R.; Tagmatarchis, N.; Benito, A. M.; Maser, W. K. Supramolecular-enhanced charge transfer within entangled polyamide chains as the origin of the universal blue fluorescence of polymer carbon dots. *J. Am. Chem. Soc.* **2018**, *140*, 12862−12869.
(33) Jia, H.; Wang, Z.; Yuan, T.; Yuan, F.; Li, X.; Li, Y.; Tan, Z. a.; Fan, L.; Yang, S. Electroluminescent Warm White Light-Emitting Diodes Based on Passivation Enabled Bright Red Bandgap Emission Carbon Quantum Dots. *Adv. Sci.* **2019**, *6*, 1900397.
(34) Qu, D.; Zheng, M.; Zhang, L.; Zhao, H.; Xie, Z.; Jing, X.; Haddad, R. E.; Fan, H.; Sun, Z. Formation mechanism and optimization of highly luminescent N-doped graphene quantum dots. *Sci. Rep.* **2014**, *4*, 5294.
(35) Wang, R.; Wang, X.; Sun, Y. One-step synthesis of self-doped carbon dots with highly photoluminescence as multifunctional biosensors for detection of iron ions and pH. *Sens. Actuators, B* **2017**, *241*, 73−79.

https://doi.org/10.1021/acsomega.2c02949
ACS Omega 2022, 7, 29952−29958